IEEE Access
Multidisciplinary | Rapid Review | Open Access Journal

Received November 25, 2017, accepted January 28, 2018, date of publication January 31, 2018, date of current version February 28, 2018.

Digital Object Identifier 10.1109/ACCESS.2018.2800095

Multi-Channel Physical Random Bits Generation Using a Vertical-Cavity Surface-Emitting Laser Under Chaotic Optical Injection

XI TANG, GUANG-QIONG XIA, ELUMALAI JAYAPRASATH, TAO DENG, XIAO-DONG LIN, LI FAN, ZI-YE GAO, AND ZHENG-MAO WU

School of Physics, Southwest University, Chongqing 400715, China

Corresponding authors: Guang-Qiong Xia (gqxia@swu.edu.cn) and Zheng-Mao Wu (zmwu@swu.edu.cn)

This work was supported in part by the National Natural Science Foundation of China under Grant 61475127, Grant 61575163, Grant 61775184, and Grant 11704316, and in part by the Fundamental Research Funds for the Central Universities of China under Grant XDJK2017C063.

ABSTRACT We experimentally demonstrate multi-channel physical random bits (PRBs) generation by utilizing chaotic outputs from two linear polarization modes in a vertical-cavity surface-emitting laser (VCSEL) under a chaotic optical injection. The polarization-resolved chaotic signal is obtained with a master-VCSEL subject to optical feedback, and then injects into a slave-VCSEL for driving its two linear polarization modes into chaotic state. We analyze the influences of injection parameters on bandwidth, complexity, and the correlation of two-channel chaotic signals. By using the two chaotic signal outputs from the slave-VCSEL under optimized parameters as entropy sources, we have obtained the PRBs at the dual-channel rate of 160 Gbits/s by adopting the *m* least significant bits extraction with logical exclusive-OR (XOR) post-processing. Further utilizing the *n*-bit cross-merging method, the PRB at a rate of 320 Gbits/s could be obtained.

INDEX TERMS Chaos, vertical-cavity surface-emitting laser, optical injection, physical random bits.

I. INTRODUCTION

The physical random bit (PRB) generators have gained much attention due to their significant potential in diverse applications including large-scale Monte Carlo simulations [1], quantum cryptography [2], secure communications [3], and lottery games. In recent years, the primary research areas relating to the PRBs generation are being focused on extracting random bits from optical stochastic processes, including photon emission noise [4]–[7], photon entanglement [8], laser phase noise [9], vacuum fluctuations [10], amplified spontaneous noise [11]–[14], and chaotic dynamics [15]–[33]. In particular, the field of chaotic dynamics in semiconductor lasers [15], [20] has received widespread attention due to the relatively strong random fluctuation of light intensity with large spectral bandwidth, which is especially suitable as an entropy source for generating PRBs.

In 2008, Uchida *et al.* have obtained PRB at a rate up to 1.7 Gbits/s by extracting from two broadband chaotic laser beams with 1-bit analog-to-digital converters (ADCs) and logical exclusive-OR (XOR) operation used [15]. Subsequently, they have generated PRB at a rate up to 2.08 Gbits/s by integrating the distributed feedback semiconductor lasers (DFB-SLs) with external optical feedback components onto a chip via photonic integration technology, which makes a significant breakthrough in miniaturization and stabilization of the PRB generation with chaos [16]. Through optimizing 1-bit quantification scheme of the entropy sources [17], [18], the rate of PRB has been improved to 4.5 Gbits/s by Wang *et al.* These demonstrations of 1-bit sampling schemes have simple and reliable structures and are easy to be implemented in hardware. However, these schemes are relatively low efficiency on the improvement in speed since the sampling process abandons large amounts of the information from the entropy sources. In 2009, Reidler *et al.* [19] proposed a method of extracting entropy source of information based on a multi-bit ADC. In this method, chaotic laser output was obtained with an optical-feedback DFB-SL system, and the light intensity was sampled and quantified by 8-bit ADC. A high-speed PRB at a rate up to 12.5 Gbits/s has been obtained by implementing XOR operation and m least significant bits (m-LSBs) extraction on the initial bit sequences. In addition, PRBs at a rate of 300 Gbits/s have

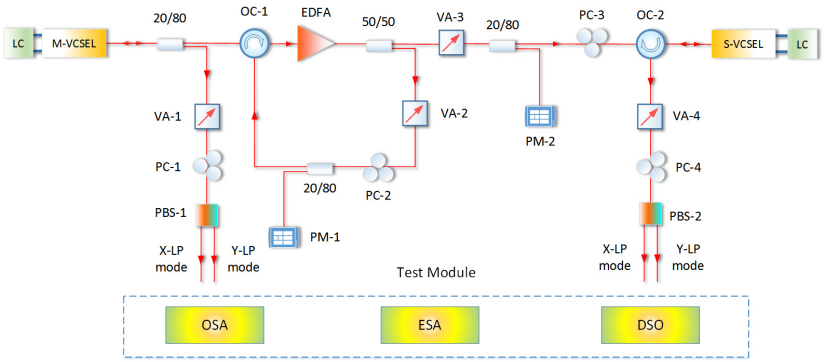

FIGURE 1. Schematic diagram of the experimental setup. LC: laser controller, M-VCSEL: master-VCSEL, S-VCSEL: slave-VCSEL, VA: variable attenuator, PC: polarization controller, OC: optical circulator, PM: power meter, PBS: polarizing beam splitter, EDFA: erbium-doped optical fiber amplifier, OSA: optical spectrum analyzer, ESA: electronic spectrum analyzer, DSO: Digital Storage Oscilloscope.

also been subsequently obtained by continuously employing a multistage differential processing scheme [20]. Since then, enormous efforts have been devoted to optimize the entropy sources and improve the sampling and quantification method in multi-bit ADC schemes. For example, through introducing polarization-rotated optical-feedback to a semiconductor laser, a simple and robust fiber-based chaotic entropy source was obtained [21]; in order to avoid chaotic entropy source possessing time-delay signature, chaotic entropy source with optical feedback SL was replaced by chaotic entropy source with optically injected SL [22]; for enhancing the chaotic bandwidth of optical feedback SLs chaotic systems, extra optical injection was introduced into the systems [23]–[25]. Besides, fiber ring cavity semiconductor laser was also used to obtain chaotic entropy for supplying high dimension chaotic signals for generating PRB [26], and furthermore, photonic integrated devices [27], [28] were utilized to generate robust high-quality chaotic signals as entropy sources. In the other hand, oversampling [22] and bit-order-reversed [24] methods have been utilized in post-processing for increasing the rate of PRBs generator, and all-optical sampling method [29] have been utilized to eliminate the electronic jitter bottleneck.

Although great progress has been made on high-speed chaotic-based PRBs generation, most of the existing PRB generators based on SLs entropy sources can only generate single-channel PRBs. From the viewpoint of cost and technological applications, it is necessary to develop multi-channel high-speed PRBs generators, and then we have tried in multi-channel high-speed PRBs generation by using two mutually coupling DFB-SLs as entropy sources [32], [33]. Besides, most entropy sources utilized in these PRB generators are based on DFB-SLs systems, while the chaotic outputs of VCSELs are rarely adopted as entropy sources. Only recently, the chaotic polarization fluctuations generated by a free-running vertical-cavity surface-emitting laser (VCSEL) is proposed to be as a chaotic entropy for generating single-channel PRB at high bit rates (> 100 Gb/s) [30]. In fact, VCSEL has a unique property, namely it can realize simultaneous emission of two orthogonally polarized components under appropriate parameter conditions [34]–[36]. This property could be utilized in order to produce two channels of chaotic entropy source signals. As a result, VCSELs-based entropy sources would be essentially suitable in multi-channel physical PRB generation.

In this work, by considering this key property of VCSEL and combining our previous relevant research experiences [32]–[36], we propose and demonstrate a new method for obtaining multi-channel physical PRBs. In this method, two paths of broadband chaotic entropy source signals are obtained by using chaotic optical injected VCSEL. We firstly utilize the parallel optical feedback to ensure two orthogonally polarized components of master-VCSEL emit chaotic outputs. Then, we utilize the parallel optical injection to enhance the chaotic bandwidth of the two orthogonally polarized components of the injected slave-VCSEL. The chaotic outputs of the two orthogonally polarized components are sampled and quantified as entropy sources. We report the influence of injection power and frequency detuning on the two entropy sources. We also discuss the influence of cross-correlation between the two entropy sources on the generation of higher-rate PRBs. Finally, the optimal parameter settings are detailed for simultaneously generating multi-channel and high-quality PRBs. And under the optimal parameter settings, PRBs at the dual-channel rate of 160 Gbits/s are obtained from the two entropy sources, while a PRB at a rate of 320 Gbits/s is also obtained under cross-merging operation.

II. EXPERIMENTAL SETUP

Figure 1 shows the experimental setup that consists of two VCSELs with emission wavelength at 1550 nm wave band, which are driven by ultra-low-noise laser controllers (LC, ILX-Lightwave LDC-3724C) with precise temperature control of 0.01 °C. Optical output signals from the master-VCSEL (M-VCSEL) are divided into two parts through a

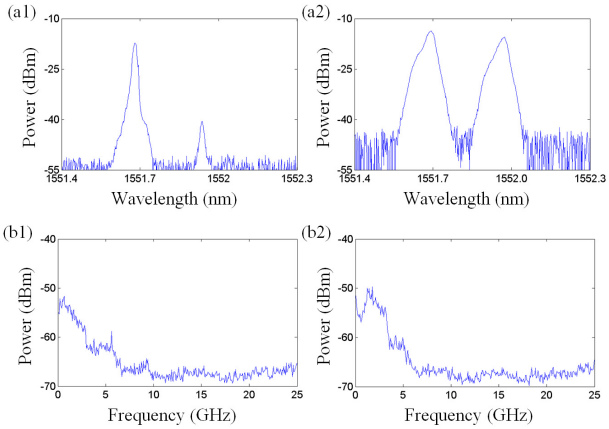

FIGURE 2. **Experimentally measured optical spectra (first row) and power spectra (second row). (a1) and (a2) are the optical spectra of M-VCSEL under free-running condition and optical feedback, respectively, and (b1) and (b2) are the corresponding power spectra of X-LP and Y-LP of the M-VCSEL under optical feedback, respectively.**

20:80 fiber coupler. The small part is sent to the test module through a variable attenuator (VA-1), and a polarization controller (PC-1), then a polarizing beam splitter (PBS-1). The test module includes an optical spectrum analyzer (OSA, Ando AQ6317), an electronic spectrum analyzer (ESA, Agilent E4407B) and a digital storage oscilloscope (DSO, Agilent DSO 91604A). The rest part is used as input to an erbium-doped fiber amplifier (EDFA) through an optical circulator (OC-1). The amplified optical signals by the EDFA are divided into two parts with a 50:50 fiber coupler. One part leads to the feedback loop via VA-2, PC-2, and OC-1, and the other part is injected into slave-VCSEL (S-VCSEL) through VA-3, PC-3, and OC-2 as the injection light. The output optical signal from S-VCSEL is sent through OC-2, VA-4, PC-4, and PBS-2 and then is split into two paths. The final two paths signals are sent to the test module. To ensure the accuracy of resolved X-linearly polarized (X-LP) and Y-linearly polarized (Y-LP) mode channels for the optical outputs of M-VCSEL and S-VCSEL under free-running, the PC-1/PBS-1 and PC-4/PBS-2 are used respectively. PC-2 and PC-3 are applied to ensure parallel optical feedback and parallel optical injection respectively. In our investigation, the feedback strength k_f is defined as the ratio of the feedback power measured by PM-1 to output power of free-running power measured at M-VCSEL. Both the feedback power and injection power is measured at power meter PM-1 and PM-2 respectively. The frequency detuning $\Delta\nu$ is defined as $\Delta\nu = \nu_M - \nu_S$, where $\nu_M(\nu_S)$ is the central frequency of M-VCSEL (S-VCSEL).

III. RESULTS AND DISCUSSION

Under free-running condition, the temperature and the bias current of the M-VCSEL are controlled at 20.90 °C and 2.7 mA respectively, where the threshold current of M-VCSEL is 1.91 mA. Figure 2(a1) is the measured optical spectrum of free-running M-VCSEL. From the diagram, one can observe that the Y-LP mode dominates meanwhile the X-LP mode is strongly suppressed, and the mode spacing between the two orthogonal polarization modes of M-VCSEL is about 0.256 nm. By introducing parallel optical feedback with a feedback strength of $k_f = 0.68$, both orthogonal polarization modes of the M-VCSEL can be simultaneously excited and driven into chaotic states as shown in Fig 2(a2). The corresponding power spectra are shown in Fig. 2(b1) and (b2), and the effective bandwidths of X-LP and Y-LP modes are 1.8 GHz and 2.3 GHz, respectively.

We set the temperature and bias current of the S-VCSEL at 21.10 °C and 3.0 mA respectively. The threshold current of S-VCSEL is 1.98 mA, and the mode spacing between the two orthogonal polarization modes of S-VCSEL is about 0.254 nm. By injecting the two orthogonal polarization modes of M-VCSEL into S-VCSEL, both orthogonal polarization modes of S-VCSEL can also be driven into chaotic states. The optical spectra of the two polarization modes of S-VCSEL for variation of the injection power at different $\Delta\nu$ ($= -15$GHz, 0GHz, 15GHz) are shown in Fig. 3. The optical spectra on the left and right columns represent the measured X-LP and Y-LP output of S-VCSEL respectively. From each row of these figures, it can be seen that the output power between the X-LP and Y-LP modes are always comparable, which indicates that two-mode coexistence phenomenon [35] of S-VCSEL are always ensured under the selected parameter conditions. Also it shows that the two output polarization modes of S-VCSEL consistently maintain in the chaotic state within the prescribed range of injection power.

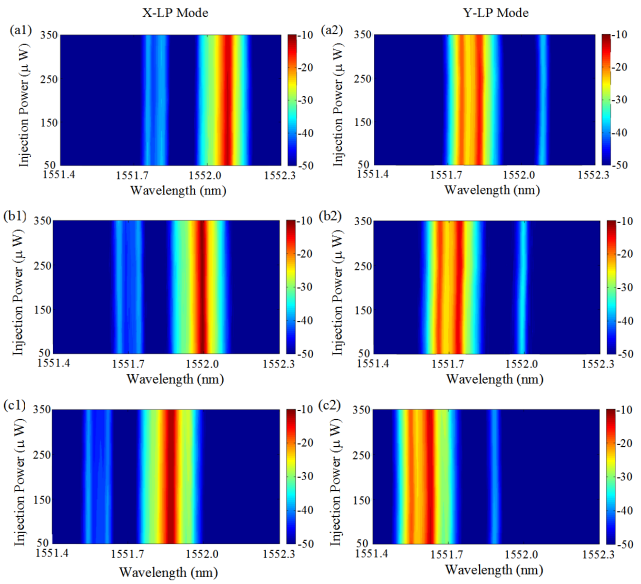

FIGURE 3. **Spectral distribution of the two polarization modes from S-VCSEL in different levels of injection power η and frequency detuning $\Delta\nu$, at fixed $k_f = 0.68$. The left (right) column of the maps corresponds to the X-LP (Y-LP) mode. (a)–(c) are obtained with frequency detuning at -15 GHz, 0 GHz, and 15 GHz, respectively. Different colors represent different values of spectral power.**

The distribution of the chaotic effective bandwidths of the two polarization modes from S-VCSEL in the described

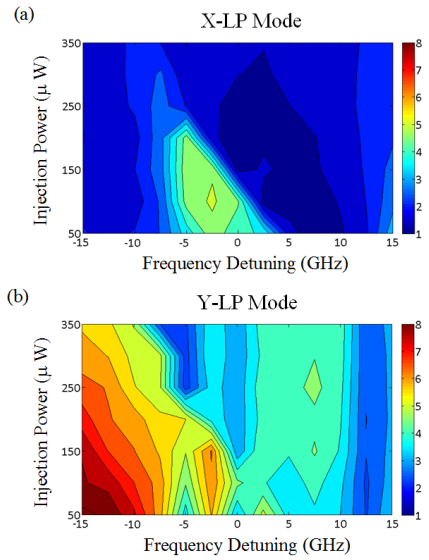

FIGURE 4. Distribution of chaotic effective bandwidth for the X-LP and Y-LP modes from S-VCSEL under the prescribed parameter space of injection power η and frequency detuning Δv.

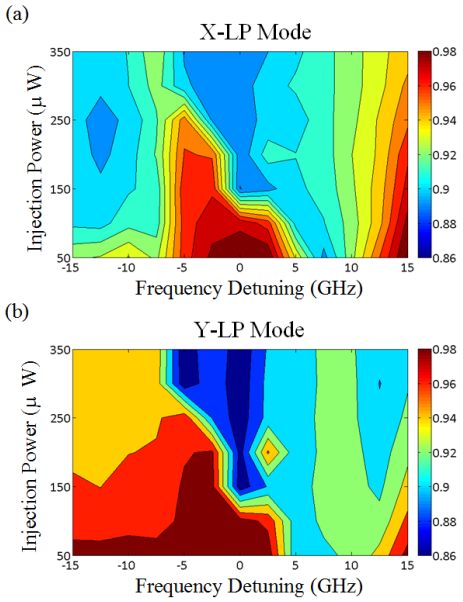

FIGURE 5. Distribution of the permutation entropy for the two polarization modes of S-VCSEL under the prescribed parameter space of η and Δv.

parameter space of η and Δv is displayed in Fig. 4, where the effective bandwidth [25] is defined as the summation of the discrete spectral segments of the chaos power spectrum accounting for 80% of the total power. In most of the parameter space regions, the chaotic bandwidth of the Y-LP mode is substantially larger than the X-LP mode. The chaotic bandwidth of the X-LP mode is lower than 3 GHz in most of the cases, and the chaotic bandwidth of the X-LP mode reaches a peak only ∼5 GHz. In the other hand, the maximum chaotic bandwidth of the Y-LP mode is as large as ∼8 GHz. The bandwidths of both X-LP mode and Y-LP mode are above 4 GHz approximately for $\Delta v \sim [-5, 0]$ GHz and $\eta \sim [50, 200]$ μW. As compared with M-VCSEL, there is a significant enhancement of bandwidths (raising to about two times) in the two polarization mode chaotic outputs of S-VCSEL within the specified parameter ranges.

In order to characterize the region of high-complexity chaotic signals, the permutation entropy [34] distribution of the two polarization mode chaotic outputs from S-VCSEL by varying η and Δv is displayed in Fig. 5. Each piont in this map means the extracted minimum values of permutation entropys with the embedding delay time varying in the neighborhoods of external cavity feedback time ∼ 150 ns under specific parameters of η and Δv. It is evident that the permutation entropy of chaotic output for the X-LP mode is higher than 0.96 in two regions of $\Delta v \sim [-5, 5$ GHz$]$, $\eta < 150$ μW, and $\Delta v \sim 15$ GHz, $\eta < 250$ μW. Similarly, the permutation entropy of the chaotic output for the Y-LP mode is usually higher than 0.96 in the region of $\Delta v \sim [-15, 5]$ GHz and $\eta < 150$ μW. Thus, the high-complexity chaotic signals, which are superior as entropy sources, could be obtained within the mentioned parameter ranges for the two polarization modes. The parameter range of high-complexity chaotic signals output for Y-LP mode is much wider than that for X-LP mode. Since the chaotic outputs of S-VCSEL are primarily applied to obtain multi-channel high-quality chaotic entropy sources, the bandwidth and complexity of output chaotic signals from the two polarization modes are demanded to be as high as possible. From the comprehensive analysis of the results of figures 4 and 5, the optimal parameter ranges for entropy source quantification and extraction are found to be $\Delta v \sim [-5, 0]$ GHz and $\eta \sim 100$ μW.

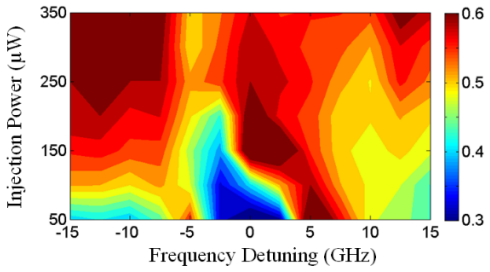

FIGURE 6. Distribution of maximum cross-correlation coefficients between the two polarization modes from S-VCSEL for the prescribed parameter space of η and Δv. The cross-correlation coefficients are taken into absolute values and different colors represent the different values.

The maximum cross-correlation coefficients [32] distribution between the two polarization modes is illustrated in Fig. 6, where the cross-correlation coefficients are taken into absolute values. It is evident that in a major part of the distribution map, the maximum cross-correlation coefficients are greater than 0.55. However, it should be noticed when the $\eta < 150\mu$W and $\Delta v \sim [-5$GHz, 5GHz$]$, the maximum cross-correlation coefficients is found to be roughly under the value 0.4. A smaller cross-correlation is more suitable for merging

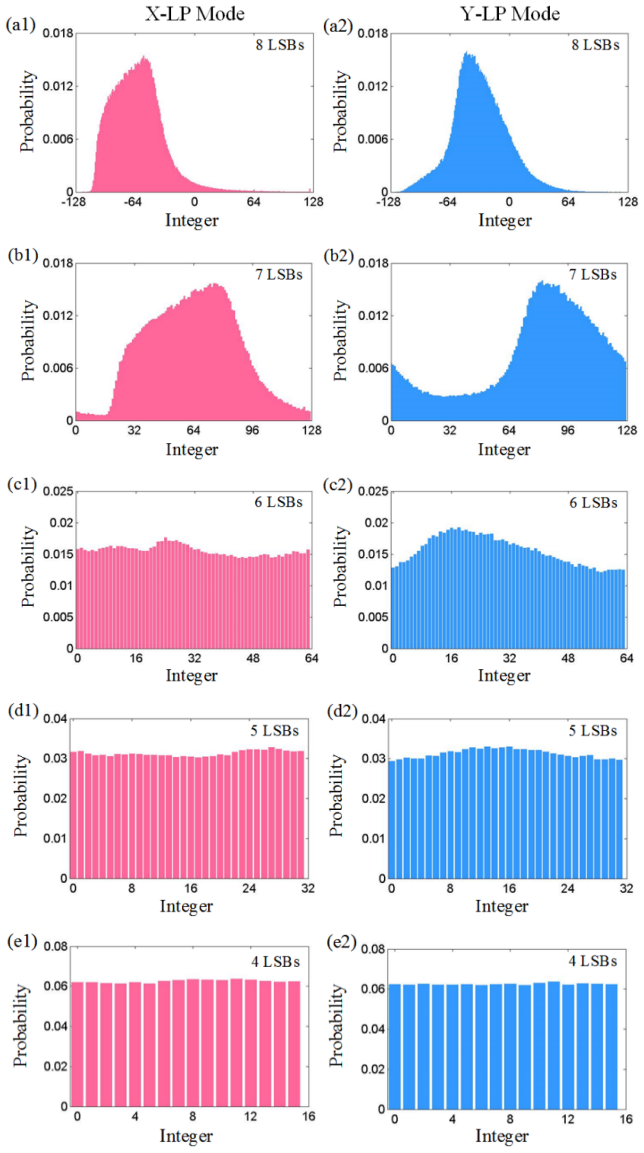

FIGURE 7. Histograms of the two polarization mode chaotic outputs from S-VCSEL after sampling quantization and LSB post-processing. (a)–(e) are the results of 8, 7, 6, 5, and 4 LSBs, respectively.

two channels of PRBs from two polarization modes together to obtain PRB with double speed rate. Comprehensively considering the multi-factors shown in Fig. 4-6, we have finally selected a group of optimal parameters in order to obtain two channel chaotic entropy sources, and in our investigation it is found to be $\eta = 100\ \mu$W and $\Delta\nu = -2.5$ GHz.

The histograms of bit sequences, which are obtained by 8-bit sampling the chaotic outputs of the two polarization modes from S-VCSEL with m-LSBs extracting, is shown in Fig. 7. For 8 LSBs as shown in Fig. 7(a), one can observe that the probability density function of the Y-LP mode chaotic output approximates a Gaussian distribution, whereas the X-LP mode chaotic output approximates a long-tailed distribution as described in [31]. Fig. 7(b)–(e) show that the distribution becomes uniform gradually with an increasing cutoff number of bits. At 4 LSBs, the distribution is almost uniform (Fig. 7e). In addition, based on information theory, the minimum entropys [33] of the two polarization modes are calculated, and the value is 5.89 for the X-LP mode and 5.94 for the Y-LP mode respectively. Thus, the maximum number of LSB for both the X-LP and Y-LP modes is 5. However, the histograms for the two polarization modes are still not uniform even 5 LSBs is applied, which means qualified PRBs cannot be obtained, and the number of LSBs have to be cut down less than 5.

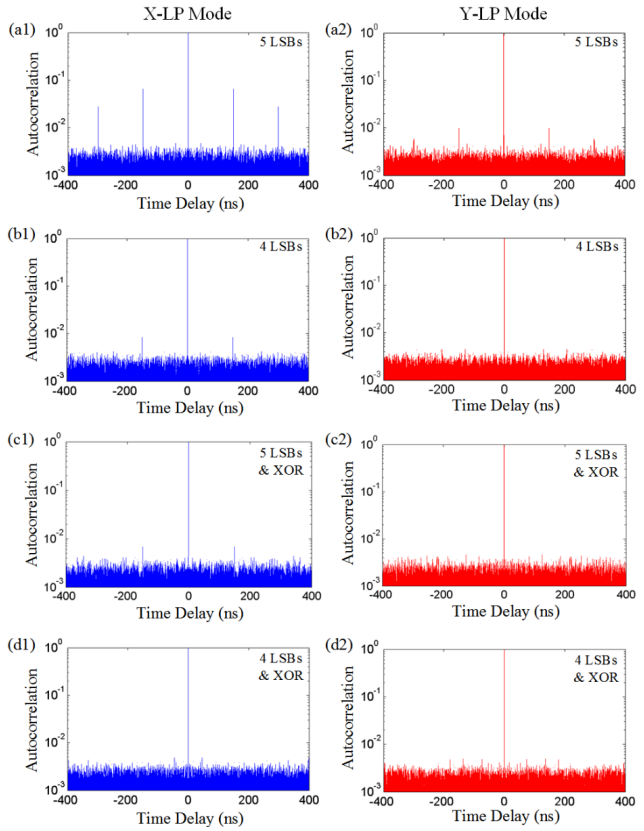

FIGURE 8. Autocorrelation results for the two polarization modes of S-VCSEL after applying m-LSBs extraction. (a) and (b) corresponds to the results after post-processing at 5 LSBs and 4 LSBs respectively. (c) and (d) shows the result at 5 LSBs and 4 LSBs after further processing by delayed XOR.

Next, we investigate the effect of post-processing on the elimination of time delay signature [32] of chaotic entropy sources, and the according results are presented in Fig. 8. As shown in Fig. 8(a), the chaotic entropy sources of the two polarization modes show an obvious time delay signatures at 5 LSBs. The time delay signatures gradually recede with an increasing cutoff number of bits, as shown in Fig. 8(b). At 4 LSBs, the time delay signatures of the Y-LP mode are completely eliminated, whereas the X-LP mode is still present. As shown in Fig. 8(c)-(d), after delayed XOR processing is further adopted [22], the time delay signatures of both polarization modes are suppressed significantly. It should be noticed that the time delay signature in X-LP

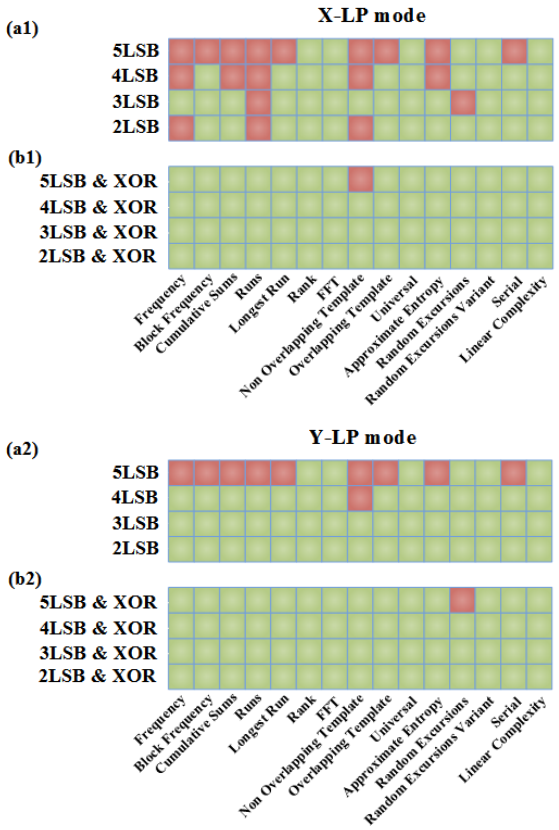

FIGURE 9. Results of the statistical test suite NIST 800-22 for PRB obtained from chaotic entropy sources of two polarization modes. The results shown in (a) are with only m-LSBs extraction, and in (b) with both m-LSBs extraction and delayed XOR processing.

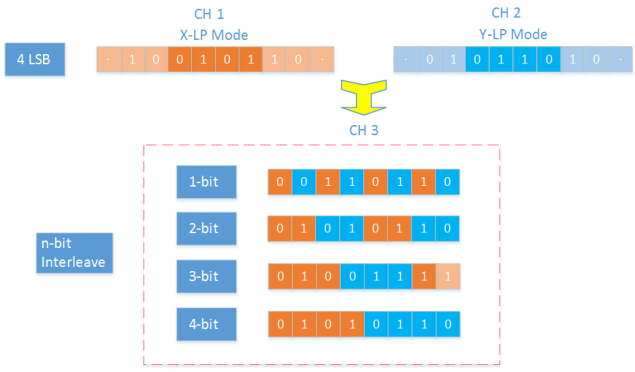

FIGURE 10. Sketch of n-bit cross-merging of dual-channel PRBs.

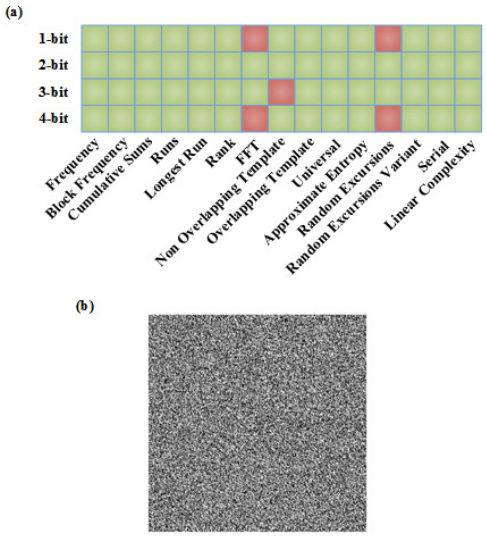

FIGURE 11. (a) NIST test results of random bit sequences acquired from the n-bit cross-merging approach; (b) 2D graph of a random bit sequence with 500 × 500 bits, where bits "1" and "0" are represented in white and black, respectively.

mode still could be observed at 5 LSBs with XOR operation. In other cases (Fig. 8(c2), (d1) and (d2)), the time delay signatures are totally eliminated. Apparently, such condition favors a superior quality of PRB generation.

The quality of PRBs obtained from the simple (m-LSBs extracting) and classical (m-LSBs extracting and delayed XOR) post-processing techniques is shown in Fig. 9. The results are described by the statistical test suite NIST 800-22 based on 1000 random bit samples with 1-Mbit length. Fig. 9(a) shows that by applying m-LSBs extracting alone, the random bit sequence from the Y-LP mode at 3 LSBs meets all 15 test requirements of NIST. Based on the property of entropy sources obtained, the sampling rate is carefully considered and is set at 40 GHz, and then the PRB rate of the Y-LP mode is $3 \times 40 = 120$ Gbits/s. Even at 2 LSBs, the random bit sequence from the X-LP mode does not meet all 15 test requirements of NIST. We believe that, comparing with Y-LP mode, the poor quality of random bit sequence from the X-LP mode is the result of the undesirable probability density function as well as the more evident of time delay signatures after m-LSBs extracting. In contrast to the above argument, Fig. 9(b) shows that after the addition of delayed XOR processing, the random bit sequences from both polarization modes can meet all 15 test requirements of NIST at 4 LSBs. Under this condition, we could obtain PRBs at dual-channel parallel bit rate of 160 Gbits/s (4 bit × 40 GHz).

Since the PRBs at dual-channel bit rate of 160 Gbits/s can be acquired, the cross-merging technique is used to obtain PRB at a higher rate. Fig. 10 shows the n-bit cross-merging approach. The dual-channel PRBs are cross-merged in a specific interval of n-bits. Fig. 11(a) presents the test results of different n values. We observe that one to two NIST tests are not satisfied when n is 1, 3, or 4. When $n = 2$, the merged random bit sequence passes all NIST tests, resulting a PRB at a rate of 320 Gbits/s. Fig. 11(b) shows a two-dimensional graph composed of 500 × 500 bits of PRB. Bits "1" and "0" are shown in white and black, respectively. We also observe that there is no deterministic relationship exists between "1" and "0". And the bits "1" and "0" show generally uniform distribution, which is what we expected to obtain.

IV. CONCLUSION

In summary, we propose a technical approach to obtain multi-channel high-speed PRBs based on the injection of polarization-resolved chaotic light into VCSEL. Initially, the

dynamic evolution of the chaotic system is investigated. Under the condition of dual-mode coexistence, we investigate the evolution (i.e., bandwidth, complexity, and correlation) of the two polarization mode outputs in the parametric space of injection power and frequency detuning. On this basis, the system parameters for dual-channel chaotic entropy sources are optimized. In addition, the results of both simple and classical post-processing method are compared, and PRBs at dual-channel rate of 160 Gbits/s are obtained by using the classical post-processing technique. Finally, the n-bit cross-merging approach is discussed, and we obtain a high-speed PRB at a rate of 320 Gbits/s under the condition of 2-bit cross-merging. We believe that this proposed scheme for parallel acquisition of multi-channel PRBs based on two polarization modes of VCSEL has offered a possible path toward designing multi-channel PRB generator.

REFERENCES

[1] A. M. Ferrenberg, D. P. Landau, and Y. J. Wong, "Monte Carlo simulations: Hidden errors from 'good' random number generators," *Phys. Rev. Lett.*, vol. 69, no. 23, pp. 3382–3384, Dec. 1992.

[2] N. Gisin, G. Ribordy, W. Tittel, and H. Zbinden, "Quantum cryptography," *Rev. Modern Phys.*, vol. 74, no. 1, pp. 145–195, Mar. 2002.

[3] I. A. Glover and P. M. Grant, *Digital Communications*, 3rd ed. Dorset, Britain: Henry Ling Ltd, 2010, pp. 514–520.

[4] A. Stefanov, N. Gisin, L. Guinnard, and H. Zbinden, "Optical quantum random number generator," *J. Modern Opt.*, vol. 47, no. 4, pp. 595–598, 2000.

[5] J. F. Dynes, Z. L. Yuan, A. W. Sharpe, and A. J. Shields, "A high speed, postprocessing free, quantum random number generator," *Appl. Phys. Lett.*, vol. 93, no. 3, p. 031109, Jun. 2008.

[6] M. A. Wayne and P. G. Kwiat, "Low-bias high-speed quantum random number generator via shaped optical pulses," *Opt. Exp.*, vol. 18, no. 9, pp. 9351–9357, Jul. 2010.

[7] H. Fürst, H. Weier, S. Nauerth, D. G. Marangon, C. Kurtsiefer, and H. Weinfurter, "High speed optical quantum random number generation," *Opt. Exp.*, vol. 18, no. 12, pp. 13029–13037, Jul. 2010.

[8] M. Fiorentino, C. Santori, S. M. Spillane, R. G. Beausoleil, and W. J. Munro, "Secure self-calibrating quantum random-bit generator," *Phys. Rev. A*, vol. 75, no. 3, pp. 032334-1–032334-6, Mar. 2007.

[9] B. Qi, Y. M. Chi, H.-K. Lo, and L. Qian, "High-speed quantum random number generation by measuring phase noise of a single-mode laser," *Opt. Lett.*, vol. 35, no. 3, pp. 312–314, 2010.

[10] C. Gabriel *et al.*, "A generator for unique quantum random numbers based on vacuum states," *Nature Photon.*, vol. 4, no. 10, pp. 711–715, Oct. 2010.

[11] C. R. S. Williams, J. C. Salevan, X. Li, R. Roy, and T. E. Murphy, "Fast physical random number generator using amplified spontaneous emission," *Opt. Exp.*, vol. 18, no. 23, pp. 23584–23597, Nov. 2010.

[12] X. Li, A. B. Cohen, T. E. Murphy, and R. Roy, "Scalable parallel physical random number generator based on a superluminescent LED," *Opt. Lett.*, vol. 36, no. 6, pp. 1020–1022, 2011.

[13] A. Argyris, E. Pikasis, S. Deligiannidis, and D. Syvridis, "Sub-Tb/s physical random bit generators based on direct detection of amplified spontaneous emission signals," *J. Lightw. Technol.*, vol. 30, no. 9, pp. 1329–1334, May 1, 2012.

[14] T. Yamazaki and A. Uchida, "Performance of random number generators using noise-based superluminescent diode and chaos-based semiconductor lasers," *IEEE J. Sel. Top. Quantum Electron.*, vol. 19, no. 4, pp. 0600309-1–0600309-9, Jul. 2013.

[15] A. Uchida *et al.*, "Fast physical random bit generation with chaotic semiconductor lasers," *Nature Photon.*, vol. 2, no. 12, pp. 728–732, 2008.

[16] T. Harayama, S. Sunada, K. Yoshimura, P. Davis, K. Tsuzuki, and A. Uchida, "Fast nondeterministic random-bit generation using on-chip chaos lasers," *Phys. Rev. A*, vol. 83, no. 3, pp. 031803-1–031803-4, Mar. 2011.

[17] J. Z. Zhang *et al.*, "A robust random number generator based on differential comparison of chaotic laser signals," *Opt. Exp.*, vol. 20, no. 7, pp. 7496–7506, Mar. 2012.

[18] A. Wang, P. Li, J. Zhang, J. Zhang, L. Li, and Y. Wang, "4.5 Gbps high-speed real-time physical random bit generator," *Opt. Exp.*, vol. 21, no. 17, pp. 20452–20462, Aug. 2013.

[19] I. Reidler, Y. Aviad, M. Rosenbluh, and I. Kanter, "Ultrahigh-speed random number generation based on a chaotic semiconductor laser," *Phys. Rev. Lett.*, vol. 103, no. 2, pp. 024102-1–024102-4, Jul. 2009.

[20] I. Kanter, Y. Aviad, I. Reidler, E. Cohen, and M. Rosenbluh, "An optical ultrafast random bit generator," *Nature Photon.*, vol. 4, pp. 58–61, Jan. 2010.

[21] N. Oliver, M. C. Soriano, D. W. Sukow, and I. Fischer, "Fast random bit generation using a chaotic laser: Approaching the information theoretic limit," *IEEE J. Quantum Electron.*, vol. 49, no. 11, pp. 910–918, Nov. 2013.

[22] X.-Z. Li and S.-C. Chan, "Random bit generation using an optically injected semiconductor laser in chaos with oversampling," *Opt. Lett.*, vol. 37, no. 11, pp. 2163–2165, 2012.

[23] K. Hirano *et al.*, "Fast random bit generation with bandwidth-enhanced chaos in semiconductor lasers," *Opt. Exp.*, vol. 18, no. 6, pp. 5512–5524, Mar. 2010.

[24] Y. Akizawa *et al.*, "Fast random number generation with bandwidth-enhanced chaotic semiconductor lasers at 8 × 50 Gb/s," *IEEE Photon. Technol. Lett.*, vol. 24, no. 12, pp. 1042–1044, Jun. 15, 2012.

[25] R. Sakuraba, K. Iwakawa, K. Kanno, and A. Uchida, "Tb/s physical random bit generation with bandwidth-enhanced chaos in three-cascaded semiconductor lasers," *Opt. Exp.*, vol. 23, no. 2, pp. 1470–1490, Jan. 2015.

[26] T. Butler *et al.*, "Optical ultrafast random number generation at 1 Tb/s using a turbulent semiconductor ring cavity laser," *Opt. Lett.*, vol. 41, no. 2, pp. 388–391, Jan. 2016.

[27] L. M. Zhang *et al.*, "640-Gbit/s fast physical random number generation using a broadband chaotic semiconductor laser," *Sci. Rep.*, vol. 7, Apr. 2017, Art. no. 45900.

[28] K. Ugajin *et al.*, "Real-time fast physical random number generator with a photonic integrated circuit," *Opt. Exp.*, vol. 25, no. 6, pp. 6511–6523, Mar. 2017.

[29] P. Li *et al.*, "Real-time online photonic random number generation," *Opt. Lett.*, vol. 42, no. 14, pp. 2699–2702, Jul. 2017.

[30] M. Virte, E. Mercier, H. Thienpont, K. Panajotov, and M. Sciamanna, "Physical random bit generation from chaotic solitary laser diode," *Opt. Exp.*, vol. 22, no. 14, pp. 17271–17280, Jul. 2014.

[31] N. Li, W. Pan, S. Xiang, Q. Zhao, and L. Zhang, "Simulation of multi-bit extraction for fast random bit generation using a chaotic laser," *IEEE Photon. Technol. Lett.*, vol. 26, no. 18, pp. 1886–1889, Sep. 15, 2014.

[32] X. Tang *et al.*, "Generation of multi-channel high-speed physical random numbers originated from two chaotic signals of mutually coupled semiconductor lasers," *Laser Phys. Lett.*, vol. 12, no. 1, pp. 015003-1–015003-6, Dec. 2015.

[33] X. Tang *et al.*, "Tbits/s physical random bit generation based on mutually coupled semiconductor laser chaotic entropy source," *Opt. Exp.*, vol. 23, no. 26, pp. 33130–33141, Dec. 2015.

[34] J. J. Chen *et al.*, "Generation of polarization-resolved wideband unpredictability-enhanced chaotic signals based on vertical-cavity surface-emitting lasers subject to chaotic optical injection," *Opt. Exp.*, vol. 23, no. 6, pp. 7173–7183, Mar. 2015.

[35] T. Deng, Z.-M. Wu, and G.-Q. Xia, "Two-mode coexistence in 1550 nm VCSELs with optical feedback," *IEEE Photon. Technol. Lett.*, vol. 27, no. 19, pp. 2075–2078, Oct. 1, 2015.

[36] Z.-Q. Zhong, Z.-M. Wu, J. Song, L.-Y. Wang, T. Deng, and G.-Q. Xia, "Polarization dynamics of 1550-nm VCSELs subject to polarization-preserved FBG feedback," *IEEE Photon. Technol. Lett.*, vol. 28, no. 9, pp. 963–966, May 1, 2016.

XI TANG was born in Chongqing, China, in 1982. He received the M.Sc. degree in optics from Southwest University, Chongqing, in 2009, where he is currently pursuing the Ph.D. degree in optics. He has co-authored over 20 publications. His research interests include random number generation based on chaotic semiconductor lasers.

GUANG-QIONG XIA was born in Fushun, China, in 1970. She received the B.Sc., M.Sc., and Ph.D. degrees in optics from Sichuan University, Chengdu, China, in 1992, 1995, and 2002, respectively.

She is currently a Full Professor with the School of Physics, Southwest University, Chongqing, China. She has authored or co-authored over 140 publications, including about 100 journal papers. Her current research interests include nonlinear dynamics of semiconductor lasers, synchronization and control of chaotic semiconductor lasers, chaos secure communication based on semiconductor lasers, and microwave photonics.

ELUMALAI JAYAPRASATH was born in Tamilnadu, India, in 1988. He received the B.Sc. degree in physics from Loyola College at Chennai, Chennai, India, in 2008, and the M.Sc. and Ph.D. degrees in physics from Pondicherry University, Pondicherry, India, in 2010 and 2016, respectively. His Ph.D. thesis was on the propagation delay and synchronization of chaotic semiconductor lasers.

He is currently a Post-Doctoral Researcher with the School of Physics, Southwest University, Chongqing, China. His current research lies in the chaos synchronization of semiconductor lasers and its utilization for secure optical communications.

TAO DENG was born in Sichuan, China, in 1982. He received the B.Sc. degree in electronic information engineering and the M.Sc. degree in optics from Southwest University, Chongqing, China, in 2002 and 2005, respectively, and the Ph.D. degree in optics from Sichuan University, Chengdu, China, in 2012.

He is currently a Full Professor with the School of Physics, Southwest University. He has authored or co-authored over 30 publications. His current research interests include nonlinear dynamics of semiconductor lasers.

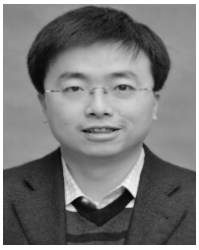

XIAO-DONG LIN was born in Chongqing, China, in 1975. He received the B.Sc., M.Sc., and Ph.D. degrees in optics from Sichuan University, Chengdu, China, in 1998, 2002, and 2012, respectively. His current researches include nonlinear dynamics of semiconductor lasers and microwave photonics.

LI FAN was born in Ziyang, China, in 1980. She received the B.Sc. degree in electronic information engineering and the M.Sc. degree in optics from Southwest University, Chongqing, China, in 2003 and 2009, respectively, where she is currently pursuing the Ph.D. degree in optics. Her research interests include microwave photonics based on nonlinear dynamics of semiconductor lasers.

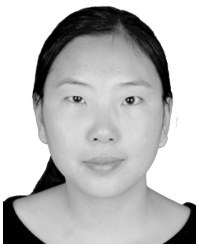

ZI-YE GAO was born in Hebei, China, in 1985. She received the B.Sc. degree in electronic science and technology and the Ph.D. degree in optics from Xidian University, Xi'an, China, in 2011 and 2016, respectively.

She is currently a Lecturer with the School of Physics, Southwest University, Chongqing, China. She has authored or co-authored over 20 publications. Her current research interests include all solid-state ultrafast lasers.

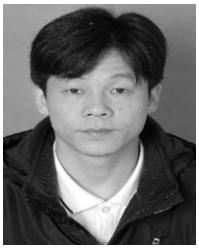

ZHENG-MAO WU was born in Wuyuan, China, in 1970. He received the B.Sc., M.Sc., and Ph.D. degrees in optics from Sichuan University, Chengdu, China, in 1992, 1995, and 2003, respectively.

He is currently a full Professor with the School of Physics, Southwest University, Chongqing, China. He has authored or co-authored over 100 publications. His current research interests include nonlinear dynamics of semiconductor lasers and their applications and chaotic semiconductor lasers and their applications.